Applied Catalysis B: Environmental 237 (2018) 660–664

Contents lists available at ScienceDirect

Applied Catalysis B: Environmental

journal homepage: www.elsevier.com/locate/apcatb

Photothermally promoted cleavage of β-1,4-glycosidic bonds of cellulosic biomass on Ir/HY catalyst under mild conditions

Bao Zhang[a,b], Jun Li[a], Lin Guo[a,c], Zhenpan Chen[a,b], Can Li[a,*,1]

[a] State Key Laboratory of Catalysis, Dalian Institute of Chemical Physics, Chinese Academy of Sciences, Dalian National Laboratory for Clean Energy, 457 Zhongshan Road, Dalian, 116023, China
[b] University of Chinese Academy of Sciences, 19A Yuquan Road, Beijing, 100049, China
[c] College of Chemistry and Molecular Sciences, Wuhan University, China

ARTICLE INFO

Keywords:
Photothermal effect
Cellulosic biomass
Hydrolysis
Ir/HY catalyst

ABSTRACT

Cellulose represents the major component of the abundant and inedible lignocellulosic biomass on earth. The valorization of cellulose into liquid biofuels and high value-added bio-based chemicals has drawn intensive attentions in recent years. However, because of the rigid structure of crystalline cellulose, the breakage of β-1,4-glycosidic bonds, the first step of cellulosic biomass utilization is still a critical challenge under mild conditions. Herein, we report the cleavage of β-1,4-glycosidic bonds of cellobiose on Ir/HY catalyst with high activity and high selectivity (> 99%) under visible light illumination at temperature not exceeding 100 °C. We found that the hydrolysis of cellobiose under mild condition is mainly owing to a cooperation effect between the Ir nanoparticles as the plasmonic photothermal source and acid catalysis of HY zeolite. This work provides a distinctive, sustainable pathway to efficiently convert cellulose to chemicals driven by solar energy under mild conditions.

1. Introduction

Cellulose is a linear, crystalline homopolymer which is composed of glucose units connected by β-1,4-glycosidic linkages. It is indiscerptible in most solvents and notoriously recalcitrant to hydrolysis due to the hierarchic networks of intramolecular and intermolecular hydrogen bonds [1–6]. Thus, efficient depolymerization of cellulose is the primary step and the entry into biorefinery schemes, which is pivotal to the utilization of cellulose [1–6]. Much endeavor has been devoted to developing efficient catalysts like homogeneous acids and cellulases to break the linkage bonds in cellulose [7–16]. However, the drawbacks such as reactor corrosion and waste disposal significantly circumscribe practical applications of homogeneous acid catalyst [7–16]. Although, enzymatic hydrolysis is an environmentally friendly process, unfortunately, impurity inhibition and high cost of cellulases limit its large-scale application [7–16]. To tackle the aforementioned obstacles, solid acid catalysts such as H-form zeolites and acid resins, have been employed for cellulose hydrolysis, recently [7–16]. However, it is an energy cost process because the reaction was usually conducted in water at high temperature and high pressure [7–16]. Therefore, it is now urgent to develop the process for efficient conversion of cellulose under mild conditions.

Solar energy driven conversion of cellulose has been considered as one of the most promising routes for the production of chemicals under mild reaction conditions [17–24]. However, due to the robust crystalline structure, only a few examples of photoreforming of rigid or pretreated cellulose have been reported [17–24]. For example, cellulose was converted to main products CO_2 and H_2 on TiO_2-based photocatalyst under UV light irradiation [17–20]. Small molecules were commonly produced in the photocatalytic process, and the distribution of the products is broad because TiO_2-based photocatalysis is non-selective in breaking the chemical bonds in cellulose [17,18]. It is highly desirable for the efficient and selective cleavage of β-1,4-glycosidic bonds in cellulosic biomass, because which is an essential prerequisite for sustainable producing high value-added chemicals, instead of producing CO_2.

Recently, photothermal effect has been demonstrated to be a versatile methodology for solar energy conversion [25–37]. It exhibits the unique capacity of metallic nanostructures, which can convert the incident light into heat through plasmonic dissipation [25,38,39]. The plasmonic effect could drastically elevate the local temperature at the nanometer scale near metal nanoparticles. Compared with conventional heating method, photothermal heating affords a rapid, straightforward, targeted heating pathway to the intended sites [27,28]. Much effort has

* Corresponding author.
E-mail address: canli@dicp.ac.cn (C. Li).
[1] Web: http://www.canli.dicp.ac.cn.

https://doi.org/10.1016/j.apcatb.2018.06.041
Received 20 March 2018; Received in revised form 13 June 2018; Accepted 15 June 2018
Available online 18 June 2018
0926-3373/ © 2018 Elsevier B.V. All rights reserved.

been devoted to investigating plasmonic metals such as Au, Ag, and Cu; however, other transition metal nanoparticles such as Ir nanoparticles have been overlooked. So it might be helpful for the biomass conversion under mild conditions by taking the advantage of the photothermal effect.

Herein, we report the cleavage of β-1,4-glycosidic bonds of cellobiose with high activity and selectivity (> 99%) on Ir/HY catalyst under visible light illumination at mild conditions. We found that the hydrolysis of cellobiose on Ir/HY catalyst with visible light irradiation is mainly contributed by the cooperation effect of acid catalysis of HY zeolite and plasmonic photothermal effect of Ir nanoparticles.

2. Experimental details

2.1. Materials

HY (Si/Al = 7), HBeta (Si/Al = 25), HY_2 (USY, Si/Al = 5.2), HY_3 (USY, Si/Al = 11) and mordenite (HMOR) zeolites were obtained from Naikai University, China. Microcrystalline cellulose was purchased from AVOCADO Research Chemicals Ltd. 1-ethyl-3-methylimidazolium chloride (EMIMCl) was provided by Lanzhou Institute of Chemical Physics, Chinese Academy of Sciences. Cellobiose was obtained from J& K Scientific. Amberlyst-15 was purchased from Dalian Melone Pharmaceutical Co., Ltd. All other chemicals were supplied from local sources and used without further purification. TiO_2 (P25, ca. 80% anatase, 20% rutile) was purchased from Degussa, and it was sintered at 300 °C for 2 h. SiO_2 (amorphous fumed), was obtained from Alfa Aesar.

2.2. Preparation of catalyst

Ir/HY-x catalyst was prepared by the impregnation method. 1 g of HY zeolite was dispersed into 165 mL of 0.1870 g/L chloroiridic acid ethanol solution. Ethanol was removed by evaporation with magnetic stirring at 80 °C. The yellow samples were dried at 80 °C for 12 h. Then, the dried solids were calcined at 250, 350, 400, 450, 500 and 600 °C for 2 h with 5 °C·min^{-1} heating rate, respectively. The resultant was reduced with H_2 at 500 °C for 2 h with 5 °C·min^{-1} heating rate, subsequently passivated in air at room temperature, achieving Ir/HY-x catalyst as black gray powders. The x is the calcination temperature (in °C). Other metals nanoparticles supported on zeolites (or P25 and SiO_2) were obtained by the same method as above. Ir/Amberlyst-15 was prepared by the impregnation method followed by H_2 reduction at 200 °C for 2 h, subsequently passivated in air at room temperature. IrO_x/HY catalyst was prepared by impregnation method by using Ir precursors. The solid was dried at 80 °C for 12 h. The as-prepared sample was calcined at 450 °C for 2 h with 5 °C·min^{-1} heating rate.

2.3. Evaluation of activity

The hydrolysis of cellobiose experiments were conducted in a 50-mL round-bottomed flask made of transparent glass with a magnetic stirrer and a rubber stopper. Typically, 50 mg cellobiose was predissolved in 4.5 g EMIMCl at 100 °C for 1 h with stirring at 300 rpm, then 50 mg Ir/HY catalyst, and 450 mg water was added in the flask. The reaction was performed at 100 °C with a silicone oil bath. The reaction solution was illuminated by a 300 W Xe lamp (PLS-SXE 300, Beijing Perfectlight Co., Ltd.) with a 420 nm-cutoff filter. Product aliquots (around 50 mg) were immediately syringed out at given time intervals. The samples were diluted with 10 g deionised water and filtered with a millipore filter (pore size 0.22 μm). The liquid phase was analyzed using an Aglient high-performance liquid chromatography (HPLC) equipped with Alltech OA-1000 Organic Acid Column (Grace), a refractive index detector and an UV detector. The mobile phase was 5 mM H_2SO_4 aqueous solution at a flow rate of 0.35 mL·min^{-1}. The column temperature was 60 °C.

2.4. Characterization methods

Crystal structures of the samples were collected on a powder X-ray diffraction (XRD) instrument Rigaku D/Max-2500/PC using Cu-Kα radiation. Optical properties were measured by an UV–vis spectrophotometer (JASCO-V550) with $BaSO_4$ as a reference. Morphologies of the samples were examined with a (Tecnai G^2 Spirit (FEI)) transmission electron microscopy (TEM) operated at an accelerating voltage of 120 kV. X-ray photoelectron spectroscopy (XPS) data were recorded on an ESCALAB 250Xi spectrometer (Thermo) and Al Ka radiation was used as the X-ray source. All data were normalized to the C 1 s peak (284.6 eV) for each sample.

The acid densities of zeolites were determined by NH_3-adsorption method. The NH_3-adsorption experiments were examined on Micrometeritics Autochem 2910 instrument. Typically, 0.08 g of sample was loaded into a quartz reactor and pretreated in He at 450 °C for 2 h. Then, the sample was cooled to 100 °C, and pulses of NH_3 were dosed in until saturation.

3. Results and discussion

Ir/HY-x catalyst was prepared by impregnation method using Ir precursors. The resultant samples were calcined at 250–600 °C in air for 2 h followed by reduction with H_2 flow at 500 °C for 2 h. The Ir/HY-x catalyst is brown powder, where x is denoted as the calcination temperature (in °C). Transmission electron microscopy in Fig. 1a shows that the ellipsoidal Ir nanoparticles with average diameters of 10.2 nm are well dispersed on the surface of HY zeolite. X-ray diffraction patterns of Ir/HY-450 catalyst display that the zeolite framework is preserved after loading Ir nanoparticles and additional peaks at 40.7° and 47.3° are the diffraction peaks of Ir nanoparticles (Fig. 1b). UV–vis spectra reveal a broad absorption band at $\lambda > 420$ nm, which is attributed to the interband and intraband transitions of Ir nanoparticles [26,40,41], in contrast to only absorption at wavelengths below 350 nm for bare HY zeolite (Fig. 1c). Fig. 1d shows X-ray photoelectronic spectrum (XPS) of Ir in Ir/HY catalyst. The binding energies of Ir 4f7/2 and Ir 4f5/2 electrons are 60.8 and 63.7 eV, respectively, which can be attributed to the Ir° state [42,43]. There are two weak peaks at 61.8 and 64.8 eV, respectively, which are assigned to the Ir^{3+} state [42,43]. This spectrum exhibits a weaker satellite peak at 66.0 eV which is consistent with the literature [42]. This result indicates that iridium is mainly in the metallic state together with a very small amount of oxidized iridium on HY zeolite. The surface of metallic Ir nanoparticles may be partially oxidized when the fresh catalyst is exposed to the air.

To facilitate the mass transfer between solid catalyst and the reactant we chose 1-ethyl-3-methylimidazolium chloride as a solvent, which can dissolve, swell crystalline cellulose [44,45]. Cellobiose which is a dimer of glucose with β-1,4-glycosidic bonds, is chosen as a model compound for the hydrolysis reaction. The reaction was performed under continuous illumination of visible light from a 300 W Xe lamp equipped with a 420 nm cut-off filter. Fig. 2 summarizes the results of the hydrolysis of cellobiose on different catalysts in the dark or under visible light irradiation. HY zeolite exhibits a low activity for the hydrolysis reaction in the dark, demonstrating that HY zeolites can activate the reactants of this reaction. Under visible light illumination, HY zeolite gives almost no increase in conversion, as HY zeolite itself shows no absorption in visible light region. When the reaction was conducted in the dark, there is no obvious difference in activity between HY zeolite with and without the presence of Ir nanoparticles. These results suggest that metal nanoparticles are not the reaction sites without light. Surprisingly, the presence of Ir nanoparticles shows the remarkable activity enhancement under visible light irradiation, achieving 2.8 times activity of that under dark. The products of hydrolysis are glucose and 5-HMF, no other products were detected. These products are derived from the breakage of β-1,4-glycosidic bonds, not from the breakage of C—C bonds suggesting that the selectivity in the

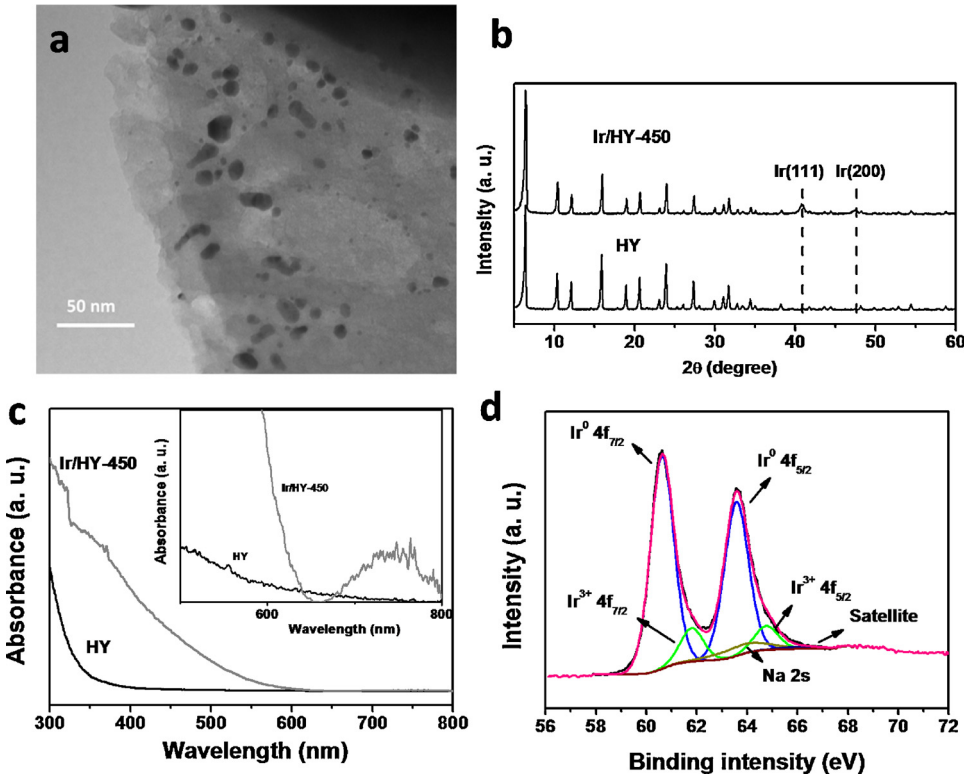

Fig. 1. (a) TEM images, (b) XRD pattern, (c) UV–vis spectra, and (d) X-ray photoelectron (XPS) spectra of Ir/HY-450 catalyst.

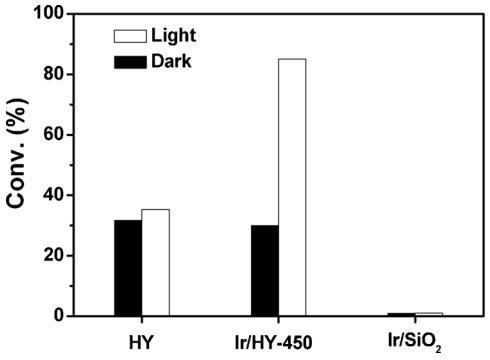

Fig. 2. The hydrolysis of cellobiose on different catalysts.
Reaction conditions: catalyst 50 mg, cellobiose 50 mg, water 450 mg, reaction temperature 100 °C, reaction time 8 h, metal loading 3 wt%, light intensity 1.1 W·cm^{-2}, wavelength range 420–800 nm.

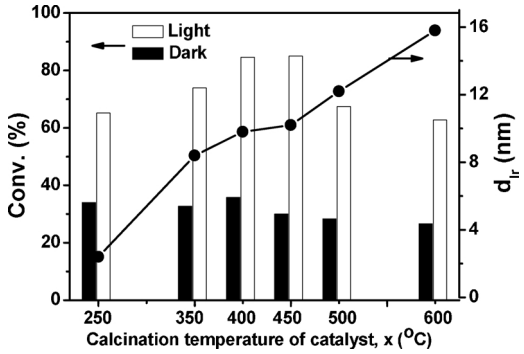

Fig. 3. The hydrolysis of cellobiose on Ir nanoparticles supported on HY zeolite. Other reaction conditions are identical to those in Fig. 2.

cellobiose hydrolysis is very high. In this work, we did not consider the decomposition of sugar such as glucose and cellobiose in the heating process. It should be pointed out that the similar conversion can be achieved only when the reaction temperature is heated to 140 °C without light irradiation (Table S1). To clarify the role of HY zeolite, Ir nanoparticles were loaded on other supports, such as SiO_2 and P25 (Table S1). However, Ir/SiO_2 or Ir/P25 catalyst is inactive (< 1%) for this reaction in the dark or under visible light irradiation (Fig. 2). These aforementioned results strongly support that both Ir nanoparticles and HY zeolite are necessary for the efficient hydrolysis of cellobiose under visible light irradiation.

To understand the effect of Ir nanoparticles on the cellobiose hydrolysis, Ir/HY catalysts were pretreated at different calcination temperatures to obtain Ir/HY catalysts with different Ir sizes. As shown in Fig. 3, the d_{Ir} for Ir/HY-250, Ir/HY-350, Ir/HY-400, Ir/HY-450, Ir/HY-500, and Ir/HY-600 catalyst are 2.4, 8.4, 9.8, 10.2, 12.2, and 15.8 nm, respectively (Figure S1). According to the literature [46,47], chloroiridic acid decomposes at around 400 °C, forming IrO_x in air; then IrO_x is reduced to metallic particles by H_2 flow at 500 °C. In the dark, these Ir/HY catalysts prepared at different calcination temperatures exhibit no obvious difference in activity. Under visible light irradiation, all the Ir/HY catalysts show the remarkably enhanced activity, and the catalyst with Ir nanoparticles size around 10 nm (Ir/HY-450 catalyst) gives the highest activity. UV–vis spectra of these Ir/HY catalysts are similar except that the absorption intensity of Ir/HY-450 catalyst is slightly higher than those of other Ir/HY catalysts (Figure S2).

After the photoreaction, no apparent changes are observed with respect to Ir nanoparticles sizes (Figure S3). There are not obvious changes in metallic Ir ratio (Figure S4). As mentioned above, there is a very small amount of IrO_x present on the Ir/HY catalyst. To further explore the role of IrO_x, IrO_x/HY catalyst was synthesized, but almost no photoactivity enhancement was observed (Table S1). There are no evident changes of particles sizes and the oxidized iridium species after the reaction (Figure S5-S6). This result proves that IrO_x is not responsible for the activity improvement under visible light irradiation.

To further understand the effect of light, light intensity and

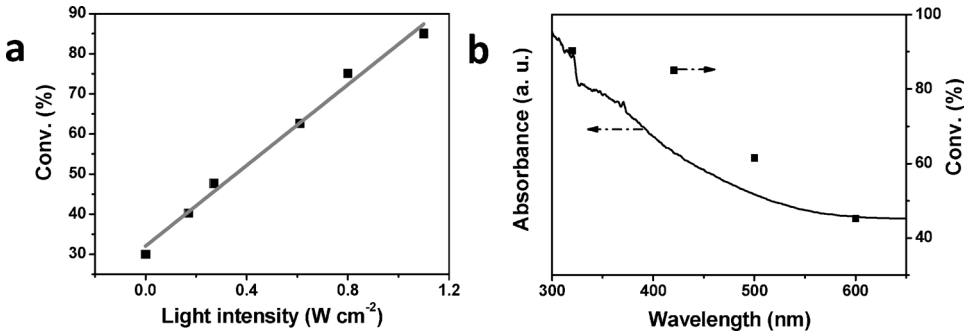

Fig. 4. The effect of light intensity (a) and the range of light wavelength (b) on the hydrolysis of cellobiose over Ir/HY-450 catalyst. Other reaction conditions are identical to those in Fig. 2.

wavelength range were investigated. As the light intensity is increased from 0.17 W·m^{-2} to 1.1 W·m^{-2}, the conversion gradually increases (Fig. 4a). There is an almost linear dependence of the conversion on the light intensity. This result confirms that the light is responsible for the enhancement in activity. Cut-off filters are used to block the light which is below the wavelength of filter threshold. With the longer cut-off wavelength used, the conversion significantly decreases (Fig. 4b). There values well match with the absorption spectrum of Ir/HY-450 catalyst. Therefore, it can be deduced that the improvement in the activity origins from the photoabsorption due to plasmonic effect of Ir nanoparticles supported on HY zeolite.

In order to gain more insight into the interaction between Ir nanoparticles and visible light on the Ir/HY catalyst under visible light irradiation, the catalyst temperature was elaborately measured (Figure S7). Under visible light irradiation, for most catalysts, the temperature increases to approximately 80–100 °C from room temperature (25 °C). In contrast, the temperature of HY zeolite in a controlled experiment is about 40 °C. For Ir/HY-450 catalyst, the highest temperature can be up to 106 °C, which is 60 °C higher than that of HY zeolite. This result clearly demonstrates that Ir nanoparticles effectively convert light into thermal energy, via so-called plasmonic thermal process [40] and thus it accelerates the catalytic hydrolysis of cellobiose. Moreover, the hydrolysis reaction is severely suppressed (< 1% conversion) at the room temperature even with visible light irradiation (Table S1). It is concluded that visible light assisted cellobiose hydrolysis on Ir/HY catalyst is mainly couple with photothermal effect.

To check whether such a phenomenon is common to other supports, Ir nanoparticles loaded on various supports were investigated, as shown in Fig. 5. Ir/SiO_2 catalyst shows very low activity even when the reaction was performed under visible light irradiation as mentioned above [48]. For HY zeolites with different Si/Al ratios, when the Si/Al

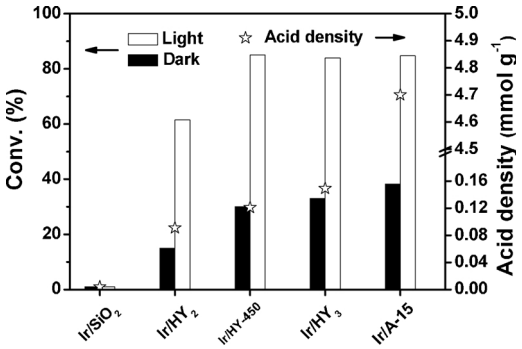

Fig. 5. The hydrolysis of cellobiose on different catalysts.
Other reaction conditions are identical to those in Fig. 2. The reaction was conducted in the presence of Ir/HY_3 catalyst at 90 °C for 8 h. A-15 is Amberlyst-15. The reaction was conducted in the presence of A-15 resin at 70 °C for 5 h. The acid density of zeolites was determined by NH_3-adsorption method. Capacity exchange of A-15 resin was provided by Melone Company.

ratios of HY zeolites is increased, the activity is enhanced in the dark. Under continuous photoirradiation, these Ir/HY catalysts sharply boost the reaction activity. In addition, Ir/HY_3 catalyst with Si/Al = 11 gives the higher performance for the hydrolysis reaction at 90 °C. Interestingly, the tendency of Si/Al ratios of HY catalysts for photothermal reaction is similar to that observed for thermal reaction. Furthermore, Amberlyst-15 resin as a commercial solid acid shows the highest activity at 70 °C, and it is more active than the other Ir catalysts. These results highlight the facts that the nature of the support has a strong influence on the hydrolysis of cellobiose. From Fig. 5, the observed activity is in the order of Ir/Amberlyst-15 > Ir/HY_3 (Si/Al = 11) > Ir/HY-450 (Si/Al = 7) > Ir/HY_2 (Si/Al = 5.2) > Ir/SiO_2 with or without visible light irradiation. It is correlated well with the acid density of the supports, indicating that the acid density of supports is directly correlated with catalytic activity. For example, SiO_2 is a weak acid [49], so it exhibits very low catalytic performance; Amberlsyt-15 resin is a strong protonic solid acid which is more favorable for the scission of the β-1,4-glucosidic bonds [49]. According to the above analysis, the Ir nanoparticles are not the active sites, responsible for the hydrolysis of cellobiose and HY zeolite can activate substrate of this reaction in the dark. These results clearly lead us to the conclusion that the acidity of the support play a vital role in the hydrolysis of cellobiose and the hydrolysis reaction is catalyzed by the acidic sites on the supports.

The hydrolysis of non-pretreated crystalline cellulose on Ir/HY_3 and Ir/Amberlsyt-15 catalysts was also investigated (Table S2). For the sake of simplicity, the sum of cellobiose, glucose and 5-HMF are defined as total products. In the dark, Ir/HY_3 catalyst only shows a low activity (8.4% yield of total products) at 90 °C, and the total products mainly consist of cellobiose. With visible light illumination, the yield of total products promptly increases to 75.3%. In comparison with previous work, reaction temperature decreases by 40 °C [50]. In addition, Ir/Amberlyst-15 resin gives 72.6% yield of total products at 70 °C under visible light irradiation (Table S3). To the best of our knowledge, there is no report on hydrolysis of cellulose over heterogeneous catalysts under such low temperature so far [10,11].

4. Conclusion

In summary, we report Ir/HY catalyst for efficient cleavage of β-1,4-glycosidic bonds of cellobiose with high activity and selectivity (> 99%) with visible light irradiation at temperature not exceeding 100 °C. We found that the Ir nanoparticles are a plasmonic component for light to thermal energy conversion and the acid sites of HY zeolite are the reaction centers. Under visible light illumination, Ir/HY catalyst exhibits a significantly promoted activity compared with that under dark conditions. Furthermore, Ir/HY catalyst is also capable of converting untreated microcrystalline cellulose to chemicals under mild conditions. The work provides a new strategy for the efficient conversion of biomass into high value-added chemicals utilizing solar energy under mild conditions.

Acknowledgements

This work was financially supported by the National Natural Science Foundation of China (NSFC, Grant No. 21473190), DICP Fundamental Research Program for Clean Energy (DICP No. M201302) and the Strategic Priority Research Program of the Chinese Academy of Sciences (Grant No. XDB17020200).

Appendix A. Supplementary data

Supplementary material related to this article can be found, in the online version, at doi:https://doi.org/10.1016/j.apcatb.2018.06.041.

References

[1] A. Corma, S. Iborra, A. Velty, Chem. Rev. 107 (2007) 2411–2502.
[2] G.W. Huber, S. Iborra, A. Corma, Chem. Rev. 106 (2006) 4044–4098.
[3] P.L. Dhepe, A. Fukuoka, ChemSusChem 1 (2008) 969–975.
[4] J.A. Geboers, S. Van de Vyver, R. Ooms, B. Op de Beeck, P.A. Jacobs, B.F. Sels, Catal. Sci. Technol. 1 (2011) 714–726.
[5] J.P. Ma, W.Q. Yu, M. Wang, X.Q. Jia, F. Lu, J. Xu, Chin. J. Catal. 34 (2013) 492–507.
[6] W.P. Deng, Q.H. Zhang, Y. Wang, Catal. Today 234 (2014) 31–41.
[7] R. Rinaldi, F. Schuth, ChemSusChem 2 (2009) 1096–1107.
[8] K. Shimizu, A. Satsuma, Energy Environ. Sci. 4 (2011) 3140–3153.
[9] P.F. Yang, H. Kobayashi, A. Fukuoka, Chin. J. Catal. 32 (2011) 716–722.
[10] Y.-B. Huang, Y. Fu, Green Chem. 15 (2013) 1095–1111.
[11] L. Hu, L. Lin, Z. Wu, S.Y. Zhou, S.J. Liu, Appl. Catal. B: Environ. 174–175 (2015) 225–243.
[12] W.P. Deng, Y.L. Wang, Q.H. Zhang, Y. Wang, Catal. Surv. Asia 16 (2012) 91–105.
[13] K. Nakajima, M. Hara, ACS Catal. 2 (2012) 1296–1304.
[14] S. Suganuma, K. Nakajima, M. Kitano, D. Yamaguchi, H. Kato, S. Hayashi, M. Hara, J. Am. Chem. Soc. 130 (2008) 12787–12793.
[15] D. Lai, L. Deng, Q. Guo, Y. Fu, Energy Environ. Sci. 4 (2011) 3552–3557.
[16] H. Kobayashi, T. Komanoya, K. Hara, A. Fukuoka, ChemSusChem 3 (2010) 440–443.
[17] A. Speltini, M. Sturini, D. Dondi, E. Annovazzi, F. Maraschi, V. Caratto, A. Profumo, A. Buttafava, Photochem. Photobiol. Sci. 13 (2014) 1410–1419.
[18] G. Zhang, C.S. Ni, X.B. Huang, A. Welgamage, L.A. Lawton, P.K.J. Robertson, J.T.S. Irvine, Chem. Commun. 52 (2016) 1673–1676.
[19] T. Kawai, T. Sakata, Nature 286 (1980) 474–476.
[20] D.I. Kondarides, V.M. Daskalaki, A. Patsoura, X.E. Verykios, Catal. Lett. 122 (2007) 26–32.
[21] M. Cargnello, A. Gasparotto, V. Gombac, T. Montini, D. Barreca, P. Fornasiero, Eur. J. Inorg. Chem. (2011) 4309–4323.
[22] M.O. Meloa, L.A. Silva, J. Braz. Chem. Soc. 22 (2011) 1399–1406.
[23] K. Shimura, H. Yoshida, Energy Environ. Sci. 4 (2011) 2467–2481.
[24] D.W. Wakerley, M.F. Kuehnel, K.L. Orchard, K.H. Ly, T.E. Rosser, E. Reisner, Nat. Energy 2 (2017) 17021.
[25] S. Linic, P. Christopher, D.B. Ingram, Nat. Mater. 10 (2011) 911–921.
[26] X.G. Meng, T. Wang, L.Q. Liu, S.X. Ouyang, P. Li, H.L. Hu, T. Kako, H. Iwai, A. Tanaka, J.H. Ye, Angew. Chem. Int. Ed. 53 (2014) 11478–11482.
[27] X.G. Meng, L.Q. Liu, S.X. Ouyang, H. Xu, D.F. Wang, N.Q. Zhao, J.H. Ye, Adv. Mater. 28 (2016) 6781–6803.
[28] S. Sarina, E.R. Waclawik, H.Y. Zhu, Green Chem. 15 (2013) 1814–1833.
[29] H.M. Liu, M. Li, T.D. Dao, Y.Y. Liu, W. Zhou, L.Q. Liu, X.G. Meng, T. Nagao, J.H. Ye, Nano Energy 16 (2016) 398–404.
[30] H.M. Liu, T.D. Dao, L.Q. Liu, X.G. Meng, T. Nagao, J.H. Ye, Appl. Catal. B: Environ. 209 (2017) 183–189.
[31] H.M. Liu, X.G. Meng, T.D. Dao, L.Q. Liu, P. Li, G.X. Zhao, T. Nagao, L.Q. Yang, J.H. Ye, J. Mater. Chem. A 5 (2017) 10567–10573.
[32] J. Ren, S.X. Ouyang, H. Xu, X.G. Meng, T. Wang, D.F. Wang, J.H. Ye, Adv. Energy Mater. (2016) 1601657.
[33] X.G. Zhang, A.J. Du, H.Y. Zhu, J.F. Jia, J. Wang, X.B. Ke, Chem. Commun. 50 (2014) 13893–13895.
[34] X.G. Zhang, X.B. Ke, H.Y. Zhu, Chem. Eur. J. 18 (2012) 8048–8056.
[35] Q. Xiao, E. Jaatinen, H.Y. Zhu, Chem. Asian J. 9 (2014) 3046–3064.
[36] X.-N. Guo, Z.-F. Jiao, G.-Q. Jin, X.-Y. Guo, ACS Catal. 5 (2015) 3836–3840.
[37] H.M. Liu, X.G. Meng, T.D. Dao, H.H. Zhang, P. Li, K. Chang, T. Wang, M. Li, T. Nagao, J.H. Ye, Angew. Chem. Int. Ed. 54 (2015) 11545–11549.
[38] P. Christopher, H. Xin, S. Linic, Nat. Chem. 3 (2011) 467–472.
[39] M.J. Kale, T. Avanesian, P. Christopher, ACS Catal. 4 (2014) 116–128.
[40] J.M. Sanz, D. Ortiz, R. Alcaraz de la Osa, J.M. Saiz, F. González, A.S. Brown, M. Losurdo, H.O. Everitt, F. Moreno, J. Phys. Chem. C 117 (2013) 19606–19615.
[41] S. Sarina, H.-Y. Zhu, Q. Xiao, E. Jaatinen, J.F. Jia, Y.M. Huang, Z.F. Zheng, H.S. Wu, Angew. Chem. Int. Ed. 53 (2014) 2935–2940.
[42] G.C. da Silva, N. Perini, E.A. Ticianelli, Appl. Catal. B: Environ. 218 (2017) 287–297.
[43] S.J. Freakley, J. Ruiz-Esquius, D.J. Morgan, Surf. Interface Anal. 49 (2017) 794–799.
[44] J.B. Binder, R.T. Raines, J. Am. Chem. Soc. 131 (2009) 1979–1985.
[45] H.L. Cai, C.Z. Li, A.Q. Wang, G.L. Xu, T. Zhang, Appl. Catal. B: Environ. 123–124 (2012) 333–338.
[46] S. Ardizzone, A. Carugati, S. Trasatti, J. Electroanal. Chem. Interfacial Electrochem. (1981) 287–292.
[47] W.J. Guang, R. Krishnan, J. Electrochem. Soc. 134 (1987) 1830–1831.
[48] M. Schulzendorf, C. Cavelius, P. Born, E. Murray, T. Kraus, Langmuir 27 (2011) 727–732.
[49] S. Van de Vyver, L. Peng, J. Geboers, H. Schepers, F. de Clippel, C.J. Gommes, B. Goderis, P.A. Jacobs, B.F. Sels, Green Chem. 12 (2010) 1560–1563.
[50] L.N. Wang, Z.Y. Zhang, L.X. Zhang, S. Xue, W.O.S. Doherty, I.M. O'Harab, X.B. Ke, RSC Adv. 104 (2015) 85242–85247.